INDUCTION MOTOR DRIVE BASED ON THE STATOR FLUX VECTOR CONTROL

Djordje Stojic, Slobodan Vukosavic

Abstract: The paper presents a new torque control algorithm for induction motor, based on the stator flux vector control. At each sampling period, the value of stator voltage is calculated to keep the stator flux equal to the reference vector, while the stator flux reference vector is calculated to keep the rotor flux amplitude constant at all operating conditions. The improved stator and rotor flux estimation algorithm is proposed, enabling robust and stable operation of the drive, even at low speeds. The induction motor torque is manipulated by variations of the flux angular velocity, enabling drive operation with fixed switching frequency and ripple-free torque in the steady state. The performance of the proposed algorithm is tested through various experimental runs, proving good behavior of the drive in the transient and steady state operating conditions.

Keywords: sensorless torque control, flux vector control, induction motor

---

Djordje Stojic (✉)
Electrical Institute INT
Golsvortijeva 13, 11000 Belgrade, Serbia and Montenegro
email: djs@ieent.org
tel: +381-11-444-2155

Slobodan Vukosavic
Electrical Engineering Faculty of Belgrade
Bulevar Kralja Aleksandra 73, 11000 Belgrade, Serbia and Montenegro

1 Introduction

The efforts in developing novel induction motor (IM) control algorithms are focused on drives with the minimum number of sensors required for operation. In recent years, a wide variety of speed sensorless solutions has been proposed, contributing performance increase at higher speeds, but failing to improve the drive behavior below 1% of the rated speed.

The concept of Direct Torque Control (DTC) [1]-[3] algorithms for the induction motor was introduced, improving significantly the torque control performance with the algorithms that achieve fast and robust torque control of IM without use of the current controllers and shaft position sensors. The DTC control strategies embody algorithms in which the voltage source inverter (VSI) switching patterns are generated directly as a function of the torque and flux errors (with the correlation between the torque, flux error, and switching states defined by means of the switching table combined with the sliding mode control strategy). The basic DTC concept with the hysteresis regulator [1]-[2] results in a very fast torque response, unforeseen in the conventional drives with a current controller in the minor loop. The nonlinear hysteresis-based control results in a high level of torque ripple and in an irregular inverter switching, with the commutation frequency dependent upon the modulation index, speed, flux, and current level. Various attempts to minimize the torque ripple and switching frequency variations where done by using the switching tables with adaptive sliding mode control [3].

Another attempt to minimize the torque chattering and switching frequency variations was introduced by the Stator Flux Vector Control (SFVC) schemes [4]-[6]. The aim of SFVC is to drive the estimated stator flux vector towards the reference value by indirect control of the inverter switching states, through PWM. The SFVC algorithms are based on various control strategies ("dead-beat", feed-forward, PI, sliding mode controllers, etc.), with the stator flux error used as the input variable. The output of SFVC scheme is fed into the Space Vector Modulator (SVM), achieving the DTC with constant switching frequency and smooth torque and flux waveforms.

Papers [4]-[6] present three different SFVC schemes, proving that the direct linear control of torque and stator flux vector enables fast torque dynamics, improved stator flux estimation at low speeds, and ripple free drive operation. The common drawback of these SFVC algorithms is that they rely on the calculation of the field vector position from the estimated stator flux vector and on the estimation of field velocity by differentiation of the calculated field vector angle. This leads to an increase of drive sensitivity to the measurement noise and to a decrease of drive performance, especially at low speeds (with poor field angle estimation). Also, SFVC drives [4] and [6] exhibit high sensitivity to the IM parameter variations, since these algorithms are designed in the deadbeat fashion.

In this paper, a novel SFVC algorithm is proposed for controlling the flux and torque of induction motor operating without shaft sensor. The improvements introduced in this SFVC algorithm include decreased sensitivity to IM parameter variations and improved the stability of drive operation, even at speeds close to zero. The increase in the drive performance is achieved by the following changes in the SFVC algorithm: implementation of a simplified feed-forward stator flux regulator with the reduced set of control parameters, direct manipulation of the field velocity (opposite to solutions which rely on the field position and field velocity estimation), and by using the closed-loop estimator of the stator and rotor flux vectors.

The proposed solution is verified through the set of experimental tests on a setup having 10 HP 4-pole industrial motor. The results obtained confirm the ability of proposed controller to ensure both torque and speed control in any practical operation condition including standstill.

2 The basic drive operating principle

In the proposed algorithm, the torque control relies on the fundamental behavior of the squirrel cage induction motor. Namely, the torque generation is proportional to the square of the rotor flux, slip frequency, and inversely proportional to the rotor resistance. Hence, the torque control loop derives the torque error and increases/decreases the speed of the field rotation. Variations of the field rotation velocity have the impact on the slip frequency that will, in turn, result in a desired torque change and steer the torque error towards zero.

The proposed flux estimator and associated controller are located in the stationary reference frame. The explicit flux control deals with the stator flux in order to achieve a faster response and boost up the robustness against changes of IM parameters. On the other hand, the stator flux reference is calculated so as to take into account the feed-forward component, related to the leakage flux. In turn, the rotor flux amplitude is guaranteed to be constant in the steady state and constant torque operating mode, contributing to the ease of the torque control through making the slip-torque relation linear. By operating in the constant torque mode, the proposed solution ensures a low torque ripple and a constant switching frequency. The algorithm requires setting a relatively small number of parameters and is simple for implementation.

Fig.1 shows the block diagram of the proposed DTC algorithm. The algorithm inputs are the reference rotor flux vector $\underline{\psi}^*_{DQ}$, reference torque T^*_e, and stator current $\underline{i}_{\alpha\beta s}$. The main control loop consists of the torque controller and block for the stator flux reference calculation. The amplitude of stator flux reference is calculated from the rotor flux and torque references, ensuring a constant rotor flux amplitude at the constant torque operating mode. The rotational frequency ω_e of reference vector $\underline{\psi}^*_{\alpha\beta s}$ is determined by using the torque PI controller, in order to drive the torque error towards zero. Consequently, the angle of stator flux reference vector $\underline{\psi}^*_{\alpha\beta s}$ is calculated by integration of ω_e.

The local inner loop, within the dotted rectangle, represents the linear stator flux controller. The flux controller is realized in the stationary reference frame, with zero error of the stator flux vector in the stationary state. The zero flux error is guaranteed by implementing feed-forward actions that compensate voltage drops across the stationary resistance and induced back-electromotiveforce (back-EMF). The stator flux regulator produces reference stator voltage vector $\underline{v}^*_{\alpha\beta s}$, fed to the PWM block. The proposed drive also includes compensation of “dead-time” effects in the three-phase AC inverter.

The DTC algorithm of Fig.1 includes a flux vector estimator. In this paper, the problems associated with flux estimation are resolved by using the closed-loop observer, with the rotor flux used as a feedback signal. The closed-loop observer introduces the significant improvement in the drive behavior, especially at low speeds. The closed-loop flux observer also resolves the problems of estimator output dc-drift, present in the flux estimators based on the back-EMF integration. The stator flux estimation is described in more details in the section that follows.

3 The flux vector estimation

The flux vector estimation uses the stator current vector and stator voltage vector as input variables. The stator voltage vector may be directly measured at the motor terminals, whereas this solution requires the electrical insulation between the power circuit and control hardware with considerable large bandwidth. On the other hand, the voltage reference values, fed to the space vector modulator, could be used instead of the voltage measurements, thus avoiding the use of expensive measurement hardware. When using the reference instead of the measured voltage value, care must be taken of the fact that the first does not represent the second to the full extent, due to distortions exhibited by the inverter nonlinearities [7]. If not compensated, effects of inverter nonlinearities are amplified, especially at low speeds and with a low level of voltage fundamental.

In this paper, voltage reference vector $\underline{v}^*_{\alpha\beta s}$ is used for the flux vector estimation, as suggested in [7]. To avoid irregular drive operation at low speeds due to inaccurate stator voltage samples, the inverter nonlinearities are compensated ("dead-time" compensation block in Fig.1) by using the algorithm proposed in [8].

The closed loop flux estimation is developed from the rotational dq frame model of IM expressed by the following equations

$$\underline{v}_{dqs} = \underline{i}_{dqs} R_s + j\omega \underline{\psi}_{dqs} + \frac{d\underline{\psi}_{dqs}}{dt}, \tag{1}$$

$$0 = \underline{i}_{DQ} R_r + j(\omega - \omega_r)\underline{\psi}_{DQ} + \frac{d\underline{\psi}_{DQ}}{dt}, \tag{2}$$

$$\underline{\psi}_{dqs} = L_s \underline{i}_{dqs} + M \underline{i}_{DQ}, \tag{3}$$

$$\underline{\psi}_{DQ} = L_r \underline{i}_{DQ} + M \underline{i}_{dqs}, \tag{4}$$

$$T = \frac{3}{2} p\left(\psi_{ds} i_{qs} - \psi_{qs} i_{ds}\right), \tag{5}$$

where p represents the number of pole pairs, ω is the reference frame angular velocity, and ω_r is the rotor angular speed. For the stationary $\alpha\beta$ reference frame, ω is equal to zero, while for the dq reference frame synchronous with the rotor flux vector, ω is equal to the flux vector angular velocity ω_e.

The stator flux could be calculated by solving differential equation (1). This type of flux estimation introduces positive current feedback into the DTC algorithm, causing unstable drive operation at low speeds. The unstabilities originate from the inaccurate value of stator resistance in (1) and nonlinearities of the inverter amplified by the positive stator current feedback.

The flux estimation can be improved by introducing negative current feedback into the calculation of flux vector. In this paper, the negative current feedback is indirectly introduced by using the closed loop flux observer. The operating principle of the closed loop flux estimation is based on feeding back the difference between the reference and estimated rotor flux vector. The difference signal is then used to correct the voltage model (1); consequently, minimizing the error of flux estimation. The difference signal also includes the negative feedback path for stator current, canceling out the bad influence of positive current feedback, present in (1), on the dynamic behavior of the drive. The behavior of the flux estimator is described by following equations

$$\underline{\hat{\psi}}_{\alpha\beta s} = \int [\underline{v}_{\alpha\beta s} - R_s \underline{i}_{\alpha\beta s} + G\,(\underline{\psi}^{*}_{\alpha\beta r} - \hat{\psi}_{\alpha\beta r})]\, dt, \tag{6}$$

$$\underline{\hat{\psi}}_{\alpha\beta r} = \frac{L_r}{M}\underline{\hat{\psi}}_{\alpha\beta s} - \frac{\sigma L_s L_r}{M}\underline{i}_{\alpha\beta s}, \tag{7}$$

where $\underline{\psi}^*_{\alpha\beta r}$ represents the rotor flux reference vector and G is the observer gain. Rotor flux reference $\underline{\psi}^*_{\alpha\beta r}$ is calculated by using rotor flux reference vector $\underline{\psi}^*_{DQ}$ in the rotational reference frame synchronous with the stator flux. Reference $\underline{\psi}^*_{DQ}$ is defined by components $\psi^*_Q = 0$ and ψ^*_D (component ψ^*_D can be freely adjusted). Reference vector $\underline{\psi}^*_{\alpha\beta r}$, is calculated from vector $\underline{\psi}^*_{DQ}$ by using the following inverse rotational transformation

$$\begin{bmatrix} \psi^*_{\alpha r} \\ \psi^*_{\beta r} \end{bmatrix} == \begin{bmatrix} \cos(\theta_e) & -\sin(\theta_e) \\ \sin(\theta_e) & \cos(\theta_e) \end{bmatrix} \begin{bmatrix} \psi^*_D \\ 0 \end{bmatrix}. \tag{8}$$

The d-axis of the rotational reference frame is in the direction of rotor flux reference vector $\underline{\psi}^*_{DQ}$. In (8), θ_e represents the angle of the rotational frame position. Since the angular velocity of the rotational reference frame is chosen to be equal to ω_e, which is set by the torque regulation, the reference frame angle is calculated as

$$\theta_e(k) = \theta_e(k-1) + K_\omega \omega(k). \tag{9}$$

The observer gain G is chosen according to the criterion that the stable drive operation is to be maintained for variations of R_s within the range of 25% around its nominal value, where this region may be extended if necessary. Since the analytical evaluation of G that matches this criterion is rather complicated, the more convenient procedure for setting of G is to tune its value on the experimental setup, in the following manner. (i) First, the value of R_s is intentionally detuned for 25% of its nominal value in equations (6) and (10). (ii) Then, for the detuned value of R_s, the value of G is increased until the stable drive operation is obtained. (iii) Finally, the value of R_s in equations (6) and (10) is returned to its nominal value, after proper value of parameter G is chosen in step (ii). By using the above three-step procedure, the appropriate value of observer gain G is achieved, which guaranties the stable drive operation with respect to an undesirable influence of stator resistance variations.

The flux observer, eqns. (6)-(7), enables stable drive operation, even at very low speeds. It makes drive less sensitive to variations of the drive parameters and nonlinearities of the voltage inverter.

4 The stator flux regulator

The stator flux regulator determines the stator voltage reference value, fed into the PWM block. The voltage value is calculated in order to achieve the stator flux equal to reference vector $\underline{\psi}^*_{\alpha\beta s}$ within a finite settling time. In doing so, the control is designed to achieve the zero flux error in less then three sampling periods (settling time is $t_{st} = 2.5\ T_s$, where T_s is the digital controller sampling period, $T_s = 200$ μs).

Since the flux regulator is designed in the stationary reference $\alpha\beta$ frame, with sinusoidal variable frequency references, it is necessary to design control structure that guarantees zero error signals in the stationary state. To achieve the zero steady-state error, the feed-forward control structure is included into the stator flux regulation. Fig. 2 shows the stator flux regulator, together with the space vector pulse width modulator and dead-time compensation.

The flux regulator equation is expressed as

$$\underline{v}^*_{\alpha\beta s}(k) = R_s \underline{i}_s(k) + j\omega_e(k)\underline{\psi}^*_{\alpha\beta s}(k) + K_p[\underline{\psi}^*_{\alpha\beta s}(k) - \underline{\hat{\psi}}_{\alpha\beta s}(k)]. \tag{10}$$

The first two terms on the right hand side in (10) represent the feed-forward control actions, aimed at compensating the voltage drops across the stator resistance and stator back-EMF. Notice, the feed-forward action for the back-EMF is proportional to reference stator flux vector $\underline{\psi}^*_{\alpha\beta s}$, opposite to the existing SFVC algorithm [5] that includes feed-forward action for the back-EMF proportional to the estimated stator flux vector. Consequently, the back-EMF compensation proposed in [5] introduces the flux feedback signal with a variable gain (flux velocity ω_e) that cause undesirable variations in the controller dynamics. In (10), the variable flux feedback signal is avoided by introducing the back-EMF compensation proportional to vector $\underline{\psi}^{*}_{\alpha\beta s}$.

The first two feed-forward terms in (10) determine the steady-state value of the voltage command, which guarantees zero error for a given stator flux reference vector $\underline{\psi}^{*}_{\alpha\beta s}$. The third term in equation (10) represents the feedback control action, proportional to the stator flux error. In (10), K_p is the gain of the flux regulator and $\omega_e(k)$ represents the instantaneous stator flux velocity ($\omega_e(k)$ is determined by the outer torque control loop). Notice that in (10) only one parameter, K_p, is to be set, which makes the proposed design procedure simple for implementation.

The feed-forward term in (10), which compensates the voltage drop across the stator resistance, can be found in various SFVC algorithms [4],[5]. This feed-forward action represents the positive feedback path for the stator current, thus causing an increased sensitivity of the drive to the nonlinearities of the VSI and to variations of R_s. As it was discussed in the previous section, the problems related to the positive current feedback, inherent for basic DTC algorithms, are resolved by introducing a negative current feedback indirectly through the closed-loop stator flux estimation algorithm.

Since one of the objectives of the proposed DTC algorithm is to enable drive operation with constant rotor flux amplitude, it is necessary to calculate the adequate stator flux reference for each operating condition. By using the rotational reference frame model (1)-(5) of IM, under condition that the rotor flux vector is constant, the stator currents in the stationary state can be derived from the electromagnetic torque. Hence, for the rotor flux and torque references $\psi^{*}_{Q} = 0$, T^{*}_{e}, and ψ^{*}_{D}, the reference drive stator currents are calculated by using the following equations

$$i_{qs}^{*} = \frac{2\,L_r}{3\,p\,L_m\,\psi_D^{*}} T_e^{*}, \tag{11}$$

$$\boldsymbol{i}_{ds}^{*} = \frac{\boldsymbol{\psi}_{\boldsymbol{D}}^{*}}{\boldsymbol{L}_{\boldsymbol{m}}}, \tag{12}$$

From equations (7) and (11)-(12), the stator flux reference vector is expressed as

$$\underline{\psi}_{\alpha\beta s}^{*} = \frac{\boldsymbol{M}}{\boldsymbol{L}_{\boldsymbol{r}}} \underline{\psi}_{\alpha\beta r}^{*} + \sigma\,\boldsymbol{L}_{s}\,\underline{\boldsymbol{i}}_{\alpha\beta s}^{*}, \tag{13}$$

where vector $\underline{\psi}^*_{\alpha\beta r}$ is given by (8) and vector $\underline{i}^*_{\alpha\beta s}$ is calculated from $\underline{i}^*_{dqs}$ by using the following inverse rotational transformation

$$\begin{bmatrix} i^*_{\alpha s} \\ i^*_{\beta s} \end{bmatrix} = \begin{bmatrix} \cos(\theta_e) & -\sin(\theta_e) \\ \sin(\theta_e) & \cos(\theta_e) \end{bmatrix} \begin{bmatrix} i^*_{ds} \\ i^*_{qs} \end{bmatrix}. \tag{14}$$

In (14), the value of angle θ_e is given by equation (9).

The "dead-time" compensation is achieved by using the algorithm proposed in [8]. The compensation is based on the calculation of the volt-seconds lost in the blanking period, averaged over the switching cycle. Since the voltage distortion introduced by the blanking time is of the opposite sign of the phase current, the compensation voltage added to the commanded voltage is of the same sign as the appropriate phase current.

The proposed linear controller enables fast and robust stator flux regulation, which, together with the torque regulator, yields zero steady-state errors of the rotor flux and torque for given rotor flux and torque references.

5 The torque regulator

In the previous section, it has been shown that the control of stator flux may be performed for any operating frequency. The stator flux control is extended to the direct torque control by introduction of the linear controller that manipulates the torque by using the field velocity as a command variable.

The proposed torque regulation relies on the operating principle of the IM that the torque is directly proportional to the slip frequency and to the squared amplitude of the rotor flux. This statement is proved by the following set of equations. Namely, flux velocity ω_e represents the rate of change of rotor flux angle θ_e. Since angle θ_e is defined by

$$\theta_e = arctg \frac{\psi_{\beta r}}{\psi_{\alpha r}}, \tag{15}$$

the flux angular velocity can be calculated as

$$\omega_e = \frac{d\theta_e}{dt} = \frac{\psi_{\alpha r}\dot{\psi}_{\beta r} - \psi_{\beta r}\dot{\psi}_{\alpha r}}{\left|\underline{\psi}_{\alpha\beta r}\right|^2} \quad . \tag{16}$$

Using (2) the following relation is obtained

$$T_e = \frac{3p}{2}\frac{\left|\underline{\psi}_{\alpha\beta r}\right|^2}{R_r}(\omega_e - \omega_r) = \frac{3p}{2}\frac{\left|\underline{\psi}_{\alpha\beta r}\right|^2}{R_r}\omega_s \, , \tag{17}$$

where ω_s is slip frequency.

The estimated torque signal, used as the input to the torque regulator, is calculated by using the following equation

$$\hat{T}_e = \frac{3}{2} p\left(\hat{\psi}_{\alpha s} i_{\beta s} - \hat{\psi}_{\beta s} i_{\alpha s}\right) . \tag{18}$$

The torque controller is designed to generate both the transient and steady state components of the slip velocity. The transient component determines the settling time of torque, while the steady state component determines the torque steady state value. The PI torque controller applied is defined by the following expression

$$\omega_e(k) = \omega_e(k-1) + K_{T1}[\Delta\hat{T}_e(k) - K_{T2}\,\Delta\hat{T}_e(k-1)] \, , \tag{19}$$

where K_{T1} and K_{T2} represent the control parameters, and $\Delta\hat{T}_e(k)$ represents the torque error, $\Delta\hat{T}_e(k) = T_e^* - \hat{T}_e(k)$. The torque controller works with the sampling period of 200μs. The conventional PI regulator (19) enables a fast transient response of torque, and determines the appropriate steady state value of the flux angular velocity, which varies with the torque reference and operating speed of IM.

6 The experimental tests

The proposed control scheme has been realized as an experimental drive, consisting of IGBT inverter, digitally controlled by the hardware based on the PC-platform running a real-time control software. The SFVC drive was realized using the floating-point algorithm (including the stator flux controller, flux reference calculation, stator flux estimation, torque estimation and control, anti-windup integrators, limiters, and other diagnostic facilities), with sampling period $T_s = 200\ \mu s$.

The induction machine under test was coupled to the separately controlled DC machine, used as the dynamic break. The 4-pole squirrel cage induction motor is characterized by the following data

P = 7.5 kW,   n = 1500 rpm,   V = 220 V,   f = 50 Hz.

The steady-state and transient behavior of the drive was investigated by various sets of tests.

6.1 The steady-state operating conditions

The steady-state behaviour was investigated in different operating conditions, i.e. with locked rotor, for mid- and high-speed regions.

The drive behaviour in operating conditions involving low flux angular velocities was tested by using the locked rotor tests. Fig. 3 shows the current and torque behaviour for the locked rotor, with the rotor flux and torque set to their rated values. The stator current is sinusoidal, while the estimated torque matches the reference value. The experimental results in Fig. 3 prove that the proposed PI torque control algorithm enables zero torque-error signal in stationary state. This shows that the precise torque regulation can be achieved with simple PI control strategy, contrary to the “dead-beat” structure based on solutions ([4] and [6]) that require the knowledge of exact IM parameter values to calculate the adequate regulation commands.

Fig. 4 shows the test results for torque reference set to 0.4 pu. The current waveform exibits some distorsions, while the torque matches the set value. Since, in this experiment, the drive operates at very a low frequency, the presented results show that the proposed control algorithm keeps the machine magnetized even at zero speed.

Fig 5 presents the results for mid-speed region, with torque set to 0.4 pu and rotor speed set to 0.5 pu by DC motor coupled with IM. Fig. 6 shows torque and stator current behaviour for torque set to 0.2 pu and speed set to 0.8 pu. The experimental results in Figs. 5 and 6 show that in the mid- and high-speed regions stator current is sinusoidal with small distorsions, while torque matches the reference value.

The results presented in this subsection show that the proposed torque control technique enables the zero torque-error operation in the stationary-state in a wide range of operating speeds. This proves that zero torque-error operation can be achieved by using the proposed PI control strategy that does not require precise knowledge of motor parameters. This is an improvement compared to the existing SFVC solutions [4], [6] that require accurate knowledge of motor parameters in order to generate adeqate command values for zero torque-error operation.

6.2. The transient operating conditions

The transient behavior of the proposed DTC algorithm was investigated for locked rotor and low- and mid-speed region. Fig. 7 shows torque and stator current responses for locked rotor and for torque reference step change from 0.1 to 0.2 pu. The results show that the response time of torque for the step excitation equals 4-5 sampling periods (T_s = 200 μs), with zero steady state error signal. Moreover, the presented experimental results show that the proposed DTC algorithm has response times comparable with the ones achieved with basic DTC algorithm [1]-[2]. Also, the presented results prove that achieved torque dynamic is faster when compared to the existing SFVC strategies [4]-[6] with the torque response times above 3 ms. Fig. 8 represents torque response for a step excitation for rotor speed set to 0.2 pu, while the results in Fig. 9 correspond to the speed set to 0.4 pu. The measurements presented in

Figs. 7-9 show that the torque regulator retains the same response times in a wide range of operating speeds. These test results prove that the proposed DTC algorithm is robust in relation to rotor speed variations.

The results in Fig. 10 represent the rotor speed behavior for torque reversal, showing that rotor speed has typical "saw-tooth" waveform, without significant distortions in the speed waveform. This experiment is performed in order to enable further comparasion of the proposed algorithm with the existing SFVC drives [4]-[6]. Namely, the torque and speed measurements in Fig. 10 prove that the stability of drive operation in a low-speed region is improved, since drives [4]-[6] exhibit higher speed and torque distortions in the near-zero speed operation. This improvement is accomplished by introducing the torque control algorithm that directly calculates the value of flux velocity ω_e, contrary to the strategies [4]-[6] which use the estimated value of ω_e. This improvement enables estimated torque value to match the real torque value in a wide range of operating speeds.

7 Conclusion

A sensorless IM drive based on the stator flux vector control is presented. The SFVC algorithm is derived from the basic DTC strategies, but has the advantage of operation with fixed switching frequency and low ripple of torque and flux. The improved stator flux estimation, based on a closed-loop flux observer, enabled stable operation of drive at whole range of operating speeds and loads. The linear stator flux controller with reduced set of control parameters enabled fast stator flux response in a wide range of operating conditions. The IM torque is controlled by variations of flux angular velocity, using the linear PI control strategy, enabling fast torque control with zero steady state error and low steady state ripple. When compared to the existing SFVC algorithms, the proposed control strategy introduces several improvements: drive operation relies on the direct calculation of the flux angular velocity, which contributes to the increase of the overall stability; control algorithm does not require knowledge of the exact IM parameter values to calculate precise command signals; the drive operates with decreased level of torque distortions at low speeds; and control strategy enables faster torque dynamics when compared to he existing SFVC drives.

Several experimental tests have been carried out to verify the drive performance in the steady-state and transient operating conditions. The presented experimental results showed that the fast torque response of the basic DTC technique is preserved. They also prove that the implementation of SFVC reduces the torque and flux ripple, typical for the basic DTC strategies.

References

1. **I. Takahashi, T. Noguchi** (1986) A new quick-response and high-efficiency control strategy of an induction motor, IEEE Trans. on Industrial Applications 22(5): 820-827.

2. **M. Depenbrok** (1988) Direct Self-Control (DSC) of Inverter-Fed Induction Machine, IEEE Trans. on Power Electronics 3(4): 420-429.

3. **I. Takahashi, Y. Ohmori** (1989) High-Performance Direct Torque Control of an Induction Motor, IEEE Trans. on Industry Applications 25(2): 257-264.

4. **T. G. Habetler, F. Profumo, M. Pastorelli, L. M. Tolbert** (1992) Direct Torque Control of Induction Machines Using Space Vector Modulation, IEEE Trans. on Industry Applications 28(5): 1045-1053

5. **D. Casadei, G. Serra, A. Tani, L. Zarri, F. Profumo** (2003) Constant frequency operation of a DTC induction motor drive for electric vehicle, IEEE Trans. on Industry Applications 39(2): 476-483

6. **A.Tripathi,A.M.Khambadkone,and S.K.Panda** (2001) Space vector based,constant frequency, direct torque control and dead beat stator flux control of ac machines, IEEE International Conference on Industrial Electronics, Control, Instrumentation and Automation, IECON: 219-224.

7. **J. Holtz, J. Quan** (2002) Sensorless Vector Control of Induction Motors at Very Low Speed Using a Nonlinear Inverter Model and Parameter Identification, IEEE Trans. on Industry Applications 38(4): 1087-1095

8. **J.W. Choi and S.K. Sul** (1996) Inverter output voltage synthesis using novel dead time compensation, IEEE Trans. Power Electron. 11(2): 221–224

Figure captions

Fig. 1. The block diagram of SFVC algorithm

Fig. 2. The block diagram of stator flux regulator

Fig. 3. The estimated torque and stator current for locked rotor and nominal torque

Fig. 4. The estimated torque and stator current for locked rotor and torque set to 0.4 pu

Fig. 5. The estimated torque and stator current for speed set to 0.5 pu and torque set to 0.4 pu

Fig. 6. The estimated torque and stator current for speed set to 0.8 pu and torque set to 0.2 pu

Fig. 7. Torque and stator current responses for locked rotor and for torque reference step excitation from 0.1 to 0.2 pu

Fig. 8. Torque and stator current responses for speed set to 0.2 pu and for torque reference step excitation from 0.2 to 0.4 pu

Fig. 9. Torque and stator current responses for speed set to 0.4 pu and for torque reference step excitation from 0.2 to 0.4 pu

Fig. 10. The estimated torque and actual rotor speed for torque reversal

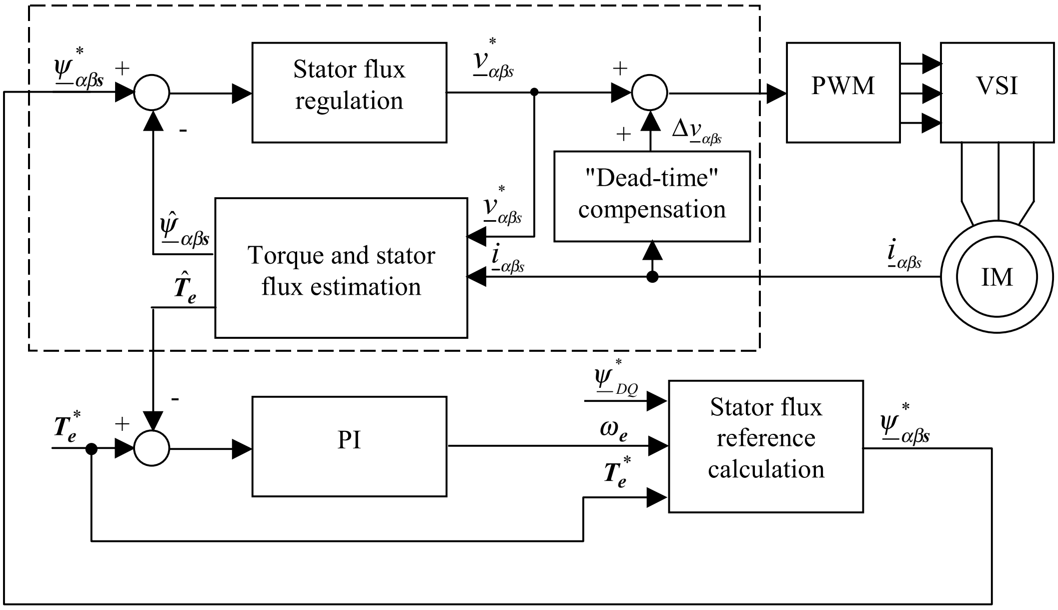

Stator flux regulation
PWM
VSI
"Dead-time" compensation
Torque and stator flux estimation
IM
PI
Stator flux reference calculation

Fig. 1

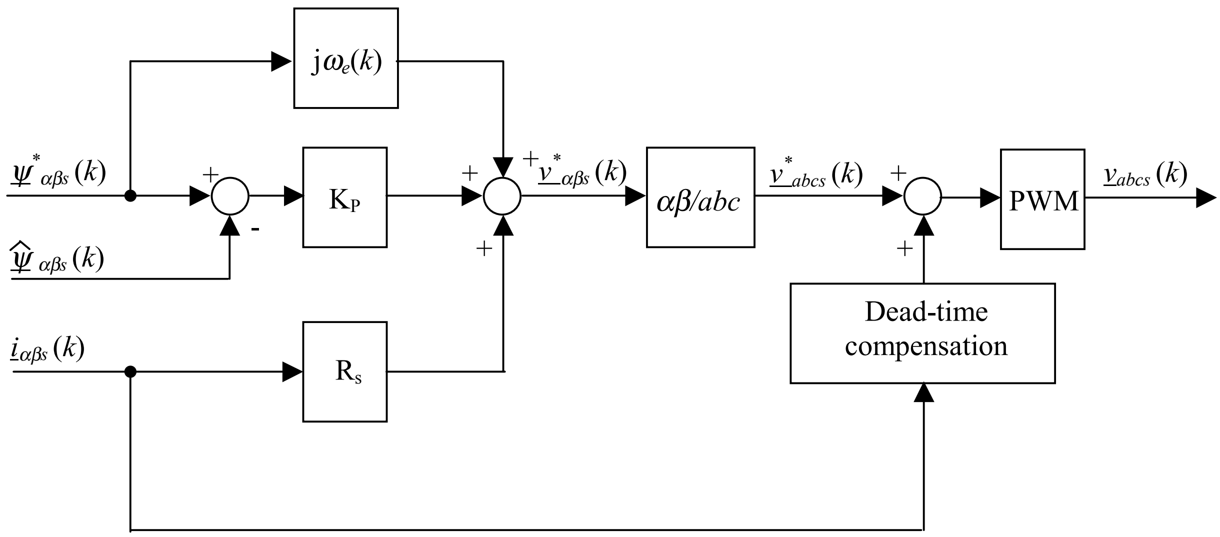

jωe(k)
ψ*αβs(k)
+
KP
+
+
v*αβs(k)
αβ/abc
v*abcs(k)
+
PWM
vabcs(k)
ψ̂αβs(k)
-
+
+
iαβs(k)
Rs
Dead-time
compensation

Fig. 2

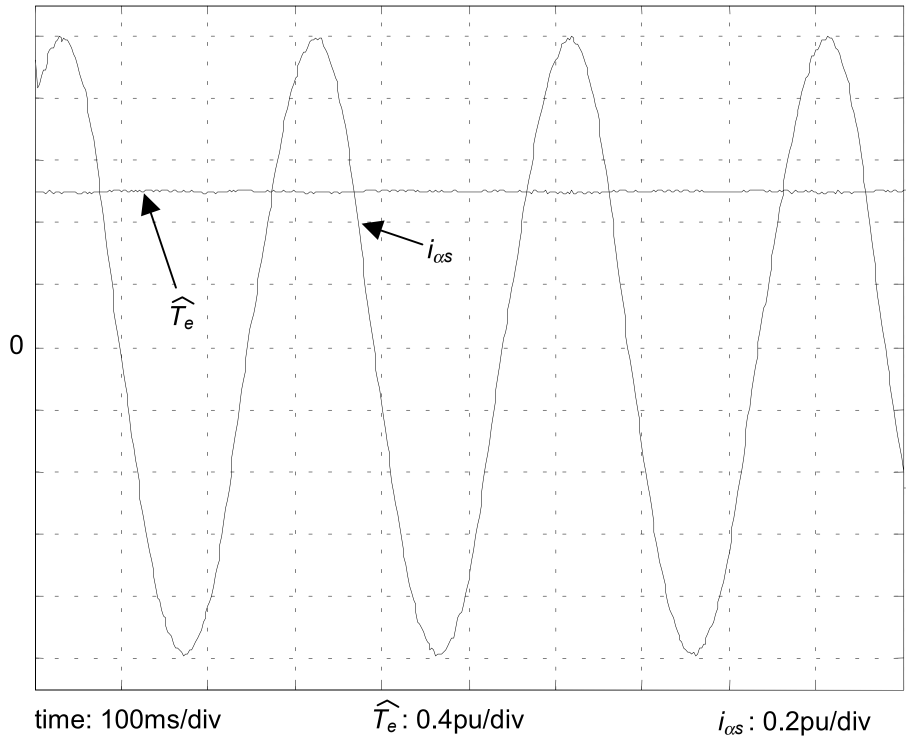

0
$\widehat{T_e}$
$i_{\alpha s}$
time: 100ms/div
$\widehat{T_e}$: 0.4pu/div
$i_{\alpha s}$: 0.2pu/div

Fig. 3

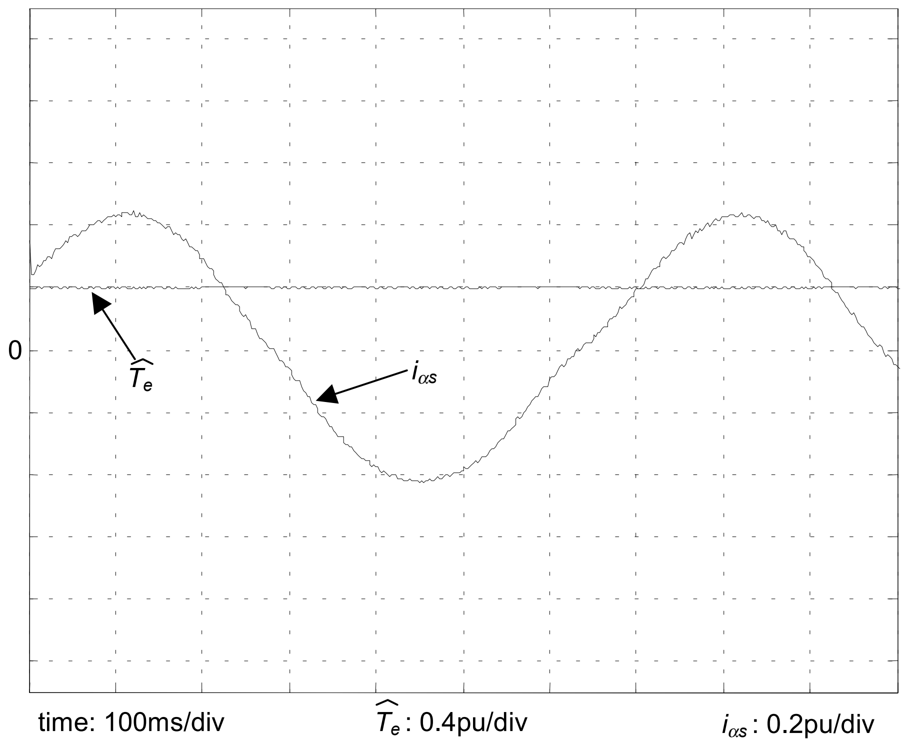
0
$\widehat{T_e}$
$i_{\alpha s}$
time: 100ms/div
$\widehat{T_e}$: 0.4pu/div
$i_{\alpha s}$: 0.2pu/div

Fig. 4

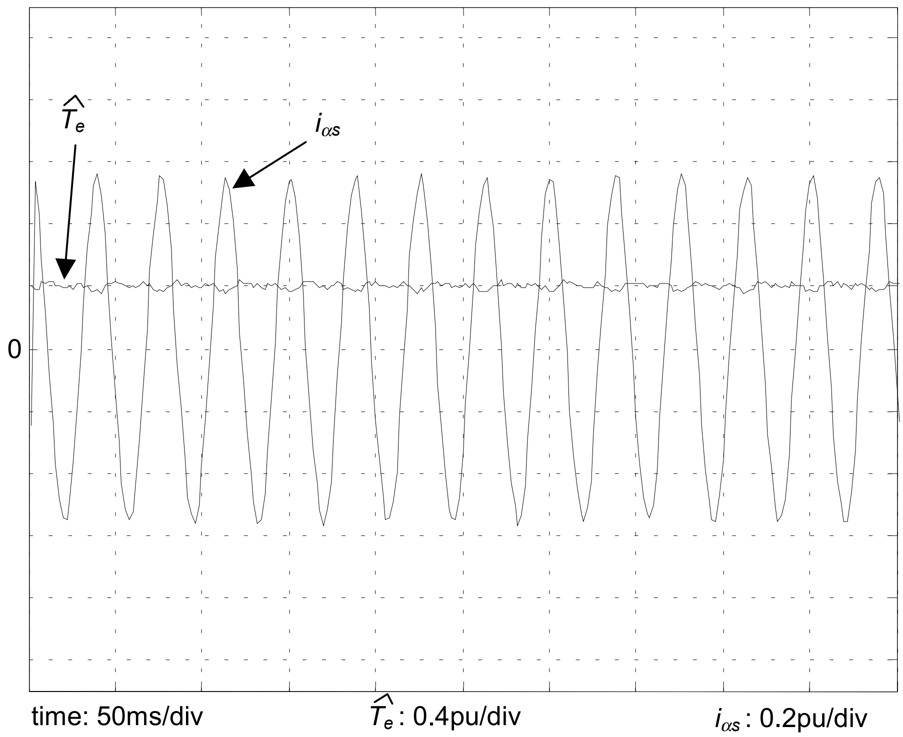
$\widehat{T_e}$
$i_{\alpha s}$
0
time: 50ms/div
$\widehat{T_e}$: 0.4pu/div
$i_{\alpha s}$: 0.2pu/div

Fig. 5

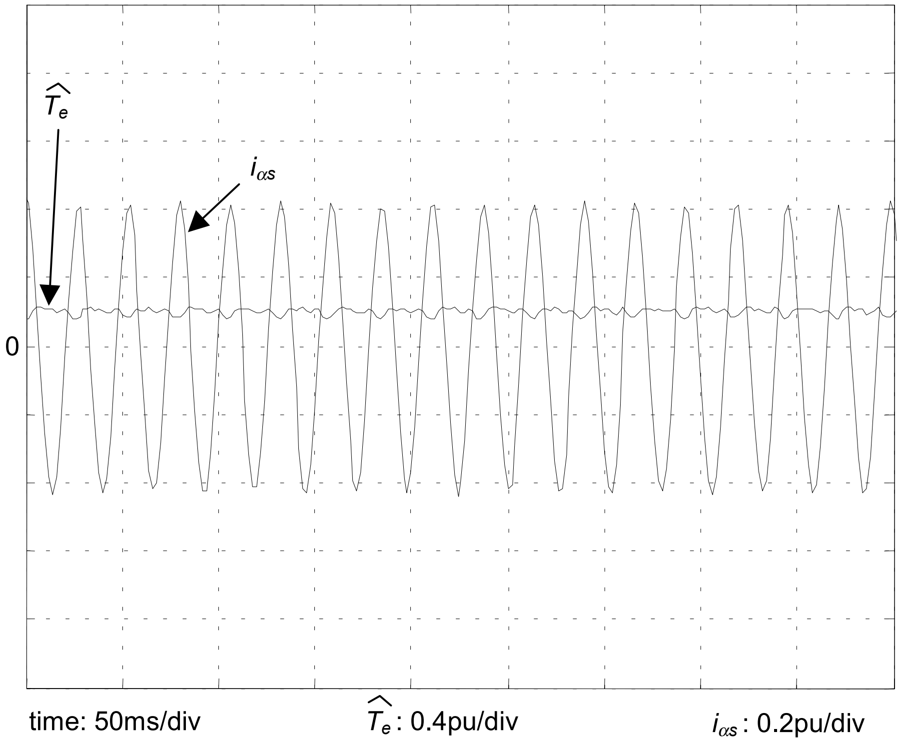

$\widehat{T_e}$
$i_{\alpha s}$
0
time: 50ms/div
$\widehat{T_e}$: 0.4pu/div
$i_{\alpha s}$: 0.2pu/div

Fig. 6

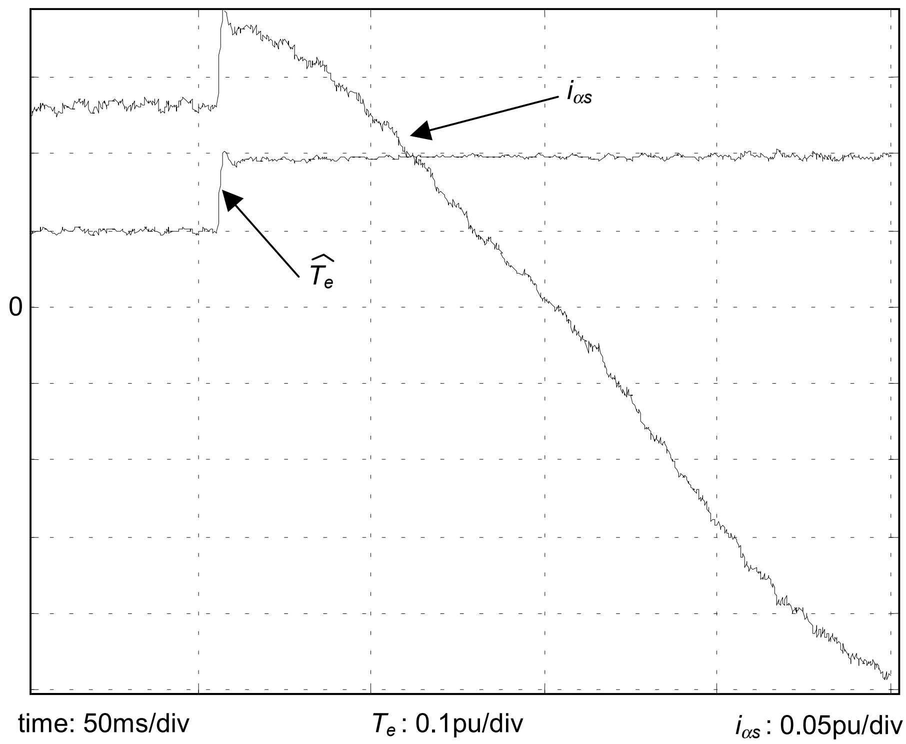
$i_{\alpha s}$
$\widehat{T_e}$
0
time: 50ms/div
T_e : 0.1pu/div
$i_{\alpha s}$: 0.05pu/div

Fig. 7

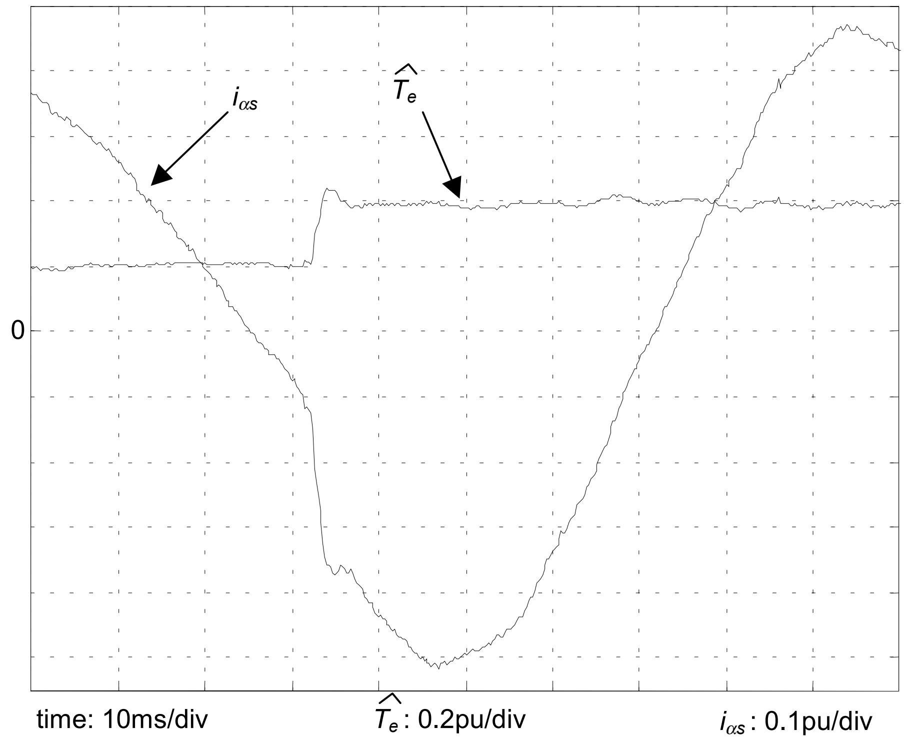
$i_{\alpha s}$
$\widehat{T_e}$
0
time: 10ms/div
$\widehat{T_e}$: 0.2pu/div
$i_{\alpha s}$: 0.1pu/div

Fig. 8

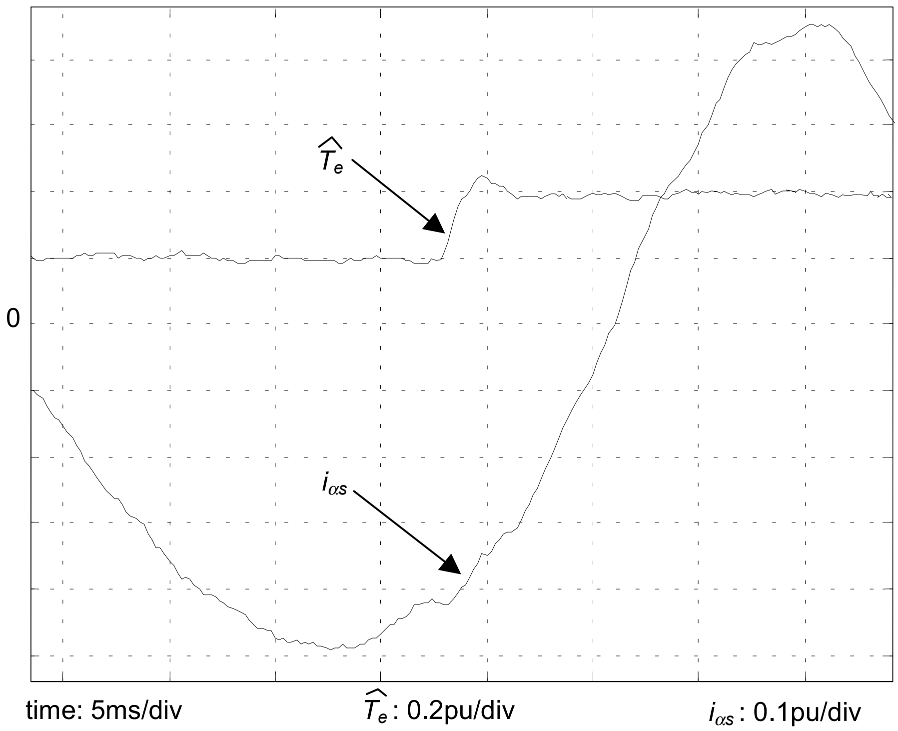

$\widehat{T}_e$
0
$i_{\alpha s}$
time: 5ms/div
$\widehat{T}_e$: 0.2pu/div
$i_{\alpha s}$: 0.1pu/div

Fig. 9

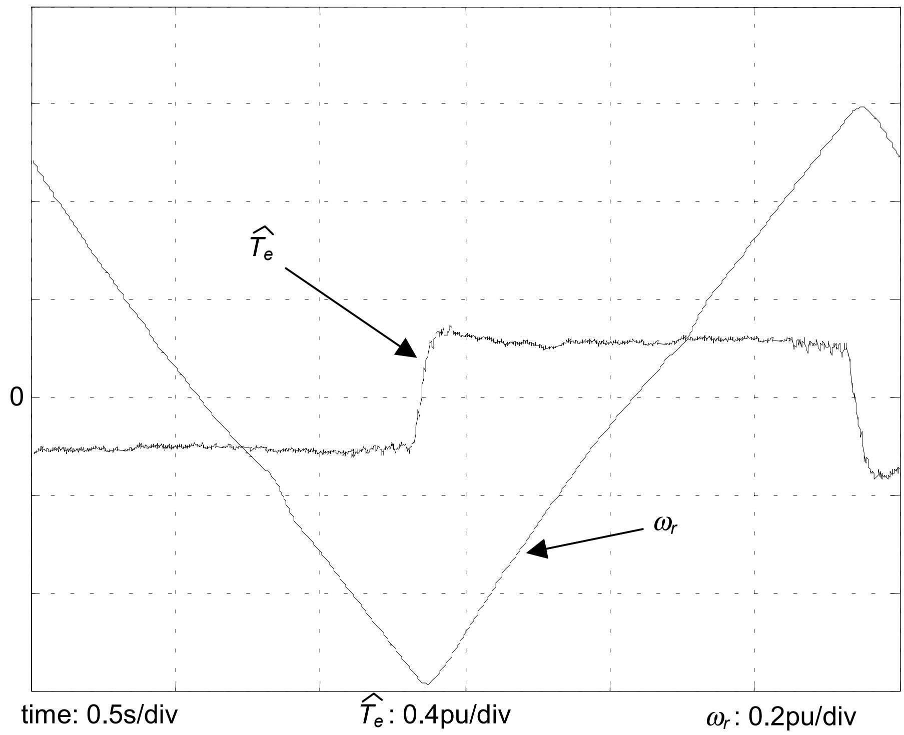

$\widehat{T_e}$
ω_r
0
time: 0.5s/div
$\widehat{T_e}$: 0.4pu/div
ω_r: 0.2pu/div

Fig. 10